PROTEINS: Structure, Function, and Genetics 51:397–408 (2003)

A Novel Shape Complementarity Scoring Function for Protein-Protein Docking

Rong Chen[1] and Zhiping Weng[1,2]*
[1]*Bioinformatics Program, Boston University, Boston, Massachusetts*
[2]*Department of Biomedical Engineering, Boston University, Boston, Massachusetts*

ABSTRACT **Shape complementarity is the most basic ingredient of the scoring functions for protein-protein docking. Most grid-based docking algorithms use the total number of grid points at the binding interface to quantify shape complementarity. We have developed a novel Pairwise Shape Complementarity (PSC) function that is conceptually simple and rapid to compute. The favorable component of PSC is the total number of atom pairs between the receptor and the ligand within a distance cutoff. When applied to a benchmark of 49 test cases, PSC consistently ranks near-native structures higher and produces more near-native structures than the traditional grid-based function, and the improvement was seen across all prediction levels and in all categories of the benchmark. Without any post-processing or biological information about the binding site except the complementarity-determining region of antibodies, PSC predicts the complex structure correctly for 6 test cases, and ranks at least one near-native structure in the top 20 predictions for 18 test cases. Our docking program ZDOCK has been parallelized and the average computing time is 4 minutes using sixteen IBM SP3 processors. Both ZDOCK and the benchmark are freely available to academic users (http://zlab.bu.edu/~rong/dock). Proteins 2003;51:397–408.**

Key words: protein docking; shape complementarity; pairwise shape complementarity; benchmark; Fast Fourier Transform

INTRODUCTION

One of the ultimate goals of genomic and proteomic projects is to determine the biological functions and cellular roles of all genes and proteins. With the rapid development of high-throughput technologies, the scientific community is flooded with sequence data. Meanwhile, structural genomics[1] has considerably accelerated the experimental determination of protein 3-Dimensional (3D) structures.[2] In addition, recent developments in proteomics technologies such as mass spectrometry, genome-scale yeast 2-hybrid, and display cloning experiments are uncovering numerous novel protein-protein interactions.[3–12] However, experimental determination of the 3D structures of protein-protein complexes has remained difficult. Knowledge of the protein complex structures can provide insights into the functions of the component proteins and can guide the design of novel molecules to regulate protein interaction networks. Thus, there is a pressing need to develop reliable and rapid protein-docking methods for predicting complex structures at a genomic scale.

There has been a wealth of research on protein-protein docking, described in several reviews.[13–19] Predictive docking methods start with the individually determined (unbound) structures of two proteins and aim to predict the complex structure, the *unbound docking* problem. Furthermore, binding site information rarely accompanies novel protein-protein interactions uncovered by proteomics. Thus, we focus on the unbound docking problem with minimal prior knowledge of the binding site. A number of methods are capable of unbound docking without assuming any binding site information.[17,20–34] All docking programs contain a scoring function that can discriminate near-native docked orientations from incorrect ones, and a search algorithm that is able to sample all possible docking orientations rapidly. To various degrees, proteins undergo conformational changes upon complex formation. Even though structural flexibility is mostly restricted to surface side chains,[35] it makes docking unbound molecules extremely difficult. Since it is infeasible to explore all possible conformations, scoring functions must be sufficiently "soft" to tolerate structural imperfections, provided that it does not lead to an increased number of false positives.

Shape complementarity is the most basic ingredient of all scoring functions for docking. As the name implies, it is a geometric descriptor, stemming from the practical observation that protein surfaces are complementary to each other at the binding interface. However, the exact formula for shape complementarity differs among docking algorithms, and can be classified into two general categories: functions based on surface curvatures or surface areas. Connolly developed a method to calculate smooth 3D contours for proteins analytically,[36,37] which has formed the basis of curvature-dependent shape complementarity since the earliest docking methods. Protein surfaces are

Grant sponsor: NSF; Grant numbers: DBI-0078194, DBI-0133834, DBI-0116574.

*Correspondence to: Zhiping Weng, Dept. of Biomedical Engineering, Boston University, 44 Cummington Street, Boston, MA 02215. E-mail: zhiping@bu.edu

Received 2 July 2002; Accepted 1 November 2002

described using critical points and surface normals, and the docking strategy is to align sets of critical points in the receptor and the ligand with opposing normals. Since this description can capture fine surface features, it works extremely well for reassembling separated components of a known complex,[38–40] and remains helpful for unbound docking.[20,29,32] The widely used small molecule docking algorithm DOCK falls within this category.[41] Shoichet and colleagues have also successfully applied DOCK to protein docking.[42,43]

A number of grid-based docking algorithms have emerged in the past decade. In the seminal work by Katchalski-Katzir and colleagues,[21] a Fast Fourier Transform (FFT)-based algorithm was introduced to explore all translational orientations rapidly. This method has been further developed by several other groups.[17,22–28] All of these methods use a surface description that does not include explicit information regarding surface curvature. Instead, a layer of grid points that surround but do not overlap with any protein atoms is computed for the receptor, and the total number of grid points in this layer that overlap any ligand grid points (which approximates buried surface area upon complexation), minus the penalty incurred by overlapping grid points that correspond to atoms in the two proteins, is the surface complementarity score (Grid-based Shape Complementarity [GSC]). Recently, we have augmented GSC with desolvation and electrostatics for unbound docking.[33]

Here, we present a novel and simple shape complementarity scoring function called Pairwise Shape Complementarity (PSC). It computes the total number of receptor-ligand atom pairs within a distance cutoff, minus a clash penalty. Unlike any of the shape complementarity functions in the above two categories, PSC is not explicitly based upon protein surface curvature or surface area. Instead, it simply rewards all close atomic contacts between the receptor and the ligand. Since neighboring atoms in one protein tend to make contacts with the same atoms in the other protein, our PSC function effectively rewards continuous surface patches at the binding site. This is an important feature for protein docking, since the interfaces of many false-positive predictions are often large but not continuous.

We have thoroughly explored the surface thickness parameter used in GSC and the distance cutoff in PSC on a benchmark of 49 test cases (version 0.0).[44] Our results indicate that PSC is much more effective than GSC for unbound docking. With optimal parameters for each method, PSC can detect near-native structures for 3 times as many test cases as GSC. FFT docking algorithms explicitly explore the entire rotational space. The receptor is fixed at the origin, and the ligand is rotated about each of its Euler angles incrementally. Therefore, the computing time scales as $1/\Delta^3$, where Δ is the angular interval. We have examined the performance of PSC at Δ of 4–15°. Results on the benchmark indicate that sampling density does not have a major impact on the ranking of the first hit. However, finer sampling consistently leads to many more hits at any given number of predictions.

Since shape complementarity sets the foundation for other scoring functions such as desolvation, electrostatics, and hydrogen bonding, our results have important implications for unbound docking. PSC is a powerful scoring function despite conformational flexibility, and can serve as an efficient primary filter before more costly evaluation criteria.

METHODS

ZDOCK

The basic search procedure in this study is similar to that in our previous study,[33] with two significant modifications:

1. *Evenly distributed Euler angles are used for the rotational search*. The Euler angle sets at several sampling intervals (Δ) have been obtained from Dr. Julie C. Mitchell. An angle set is equivalent to a uniformly distributed set of points on a projective sphere, which ensures that minimal orientations are required to cover the entire rotational space. The angular distance between any orientation and its nearest orientation, computed using the formula in Lattman,[45,46] is Δ or smaller.
2. *Only the best translational orientation is kept for every rotational orientation*. We used to keep the top 10 translational orientations for each rotation.[33] We subsequently discovered that these 10 translations are extremely similar, and keeping only the best one helped to remove false positives without affecting the ranking of the best hit.

For practical convenience, we used to take the ligand orientation as superposed on the crystal complex to be the origin of the angular sampling.[33] We subsequently noticed that this led to slightly but consistently better performance than using a random starting orientation. Thus, for all grid-based docking algorithms, it is important *not* to sample a near-native orientation deliberately. In this study, we have randomly perturbed all starting receptor and ligand orientations.

A grid spacing of 1.2 Å is used throughout this study. Also, the angular sampling density is 15° unless otherwise stated.

GSC

GSC has been described in detail in our previous publication.[33] Briefly, we obtain two functions R_{GSC} and L_{GSC} by discretizing the receptor (R) and the ligand (L) using an $N \times N \times N$ grid, with grid point (l, m, n = 1, 2, . . . , N) assigned the following value:

$$R_{GSC}(l,m,n) = \begin{cases} 1 & \text{solvent } \textit{accessible} \text{ surface layer of } R \\ 9i & \text{solvent } \textit{excluding} \text{ surface layer of } R \\ 9i & \text{core of } R \\ 0 & \text{open space} \end{cases} \quad (1)$$

$$L_{GSC}(l,m,n) = \begin{cases} 0 & \text{solvent } \textit{accessible} \text{ surface layer of } L \\ 1 & \text{solvent } \textit{excluding} \text{ surface layer of } L \\ 9i & \text{core of } L \\ 0 & \text{open space} \end{cases}$$

where $i = \sqrt{-1}$. If a protein atom has more than 1 Å^2 solvent accessible area, calculated using a water probe radius of 1.40 Å,[47] it is considered a surface atom. Otherwise, it is a core atom. The "Solvent excluding surface layer of a protein" is defined by the grid points corresponding to surface atoms. All other grid points corresponding to any core atoms are in the protein "core". "Solvent accessible surface layer" is an additional layer of grid points surrounding a protein; these grid points are adjacent to the surface atoms of a protein, but do not overlap with protein atoms. In the past, we set the thickness of this "solvent accessible surface layer" (T) at 3.4 Å, similar to the thickness of 3.5 Å used by Eisenstein and Katchalski-Katzir in the TEM-1 β-lactamase/BLIP docking challenge.[48]

GSC is computed using the following equation (o, p, and q are the number of grid points by which L is shifted with respect to R in each dimension):

$$S_{GSC}(o,p,q) = \mathrm{Re}[\sum_{l=1}^{N}\sum_{m=1}^{N}\sum_{n=1}^{N} R_{GSC}(l,m,n) \times L_{GSC}(l+o,m+p,n+q)] - \mathrm{Im}[\sum_{l=1}^{N}\sum_{m=1}^{N}\sum_{n=1}^{N} R_{GSC}(l,m,n) \times L_{GSC}(l+o,m+p,n+q)] \quad (2)$$

The above correlation can be computed rapidly using two Fourier transforms.[33]

Figure 1(a) is a 2D schematic illustration of GSC. Protein atoms are indicated by circles, with open circles for surface atoms and shaded circles for core atoms. For clarity, we set grid spacing to be the same as an atom diameter. Grid points assigned 0 have been omitted from the figure. Grid points with open circles belong to the "solvent excluding surface layer", and grid points without circles belong to the "solvent accessible surface layer". For illustration purposes, we have set the thickness of the "solvent accessible surface layer" to an atom diameter. The best ligand orientation in Figure 1(a) (indicated by a block arrow) will lead to a GSC score of 6.

PSC

The favorable component of PSC is defined as the number of receptor-ligand *atom pairs* within a distance cutoff. To account partially for different atom radii, the cutoff is defined as a parameter D plus the receptor atom radius. The unfavorable component of PSC is linearly proportional to the number of overlapping grid points between the receptor and the ligand (similar to GSC). In order to compute PSC efficiently using FFT, two complex functions, R_{PSC} and L_{PSC}, are used to describe the geometric characteristics R and L on an $N \times N \times N$ grid:

$$\mathrm{Re}[R_{PSC}(l,m,n)] = \begin{cases} \text{number of receptor atoms within (D + receptor atom radius)} & \text{open space} \\ 0 & \text{otherwise} \end{cases}$$

$$\mathrm{Re}[L_{PSC}(l,m,n)] = \begin{cases} 1 & \text{if this grid is the nearest grid of a ligand atom} \\ 0 & \text{otherwise} \end{cases}$$

$$\mathrm{Im}[R_{PSC}(l,m,n)] = \mathrm{Im}[L_{PSC}(l,m,n)] = \begin{cases} 3 & \text{solvent } \textit{excluding} \text{ surface of the protein} \\ 9 & \text{protein core} \\ 0 & \text{open space} \end{cases} \quad (3)$$

where Re[ ] and Im[ ] denote the *real* and *imaginary* parts of a complex function.

The final PSC scoring function is computed using a correlation function between R_{PSC} and L_{PSC}:

$$S_{PSC}(o,p,q) = \mathrm{Re}[\sum_{l=1}^{N}\sum_{m=1}^{N}\sum_{n=1}^{N} R_{PSC}(l,m,n) \cdot L_{PSC}(l+o,m+p,n+q)], \quad (4)$$

where ligand L is translated with respect to receptor R by o, p, and q grid points in each dimension. For each ligand rotation, the above correlation function with all possible translations can be evaluated using only two Fourier Transforms, provided the Fourier Transform of R_{PSC} is pre-computed. Details of the FFT-based search algorithm can be found in several articles.[21,33]

In Equations [3] and [4], Im[R_{PSC}] and Im[L_{PSC}] are used to compute the unfavorable component of PSC. A core-core, surface-core, or surface-surface grid point overlap results in a penalty of $-9*9 = -81$, $-3*9 = -27$, and $-3*3 = -9$ respectively. Overlaps involving surface grid points are penalized only moderately, which allows PSC to tolerate some structural flexibility. Re[R_{PSC}] and Re[L_{PSC}] are used to compute the favorable component of PSC. Re[R_{PSC}] denotes the number of receptor atoms within the distance cutoff of each grid point in the open space, and Re[L_{PSC}] records the nearest grid point for each ligand atom. The multiplication of these two terms results in the total number of receptor/ligand atom pairs within the distance cutoff. Equation [4] computes both the favorable and unfavorable components of PSC, and sums them into one score, with a higher score indicating better shape complementarity.

Figure 1(b) is a 2D schematic illustration for computing PSC. Similar to Figure 1(a), protein atoms are shown in circles, with open circles indicating surface atoms and shaded circles indicating core atoms. Unlike Figure 1(a), however, here we do not define the "solvent accessible surface layer" and any grid point that does not correspond to an atom is in the "open space". For grid points in the open space of R_{SC}, we record the total number of receptor atoms within a distance cutoff. For illustration purposes, we have defined the cutoff to be 1.5 times atom diameters, which allows atoms occupying diagonal grid points to be

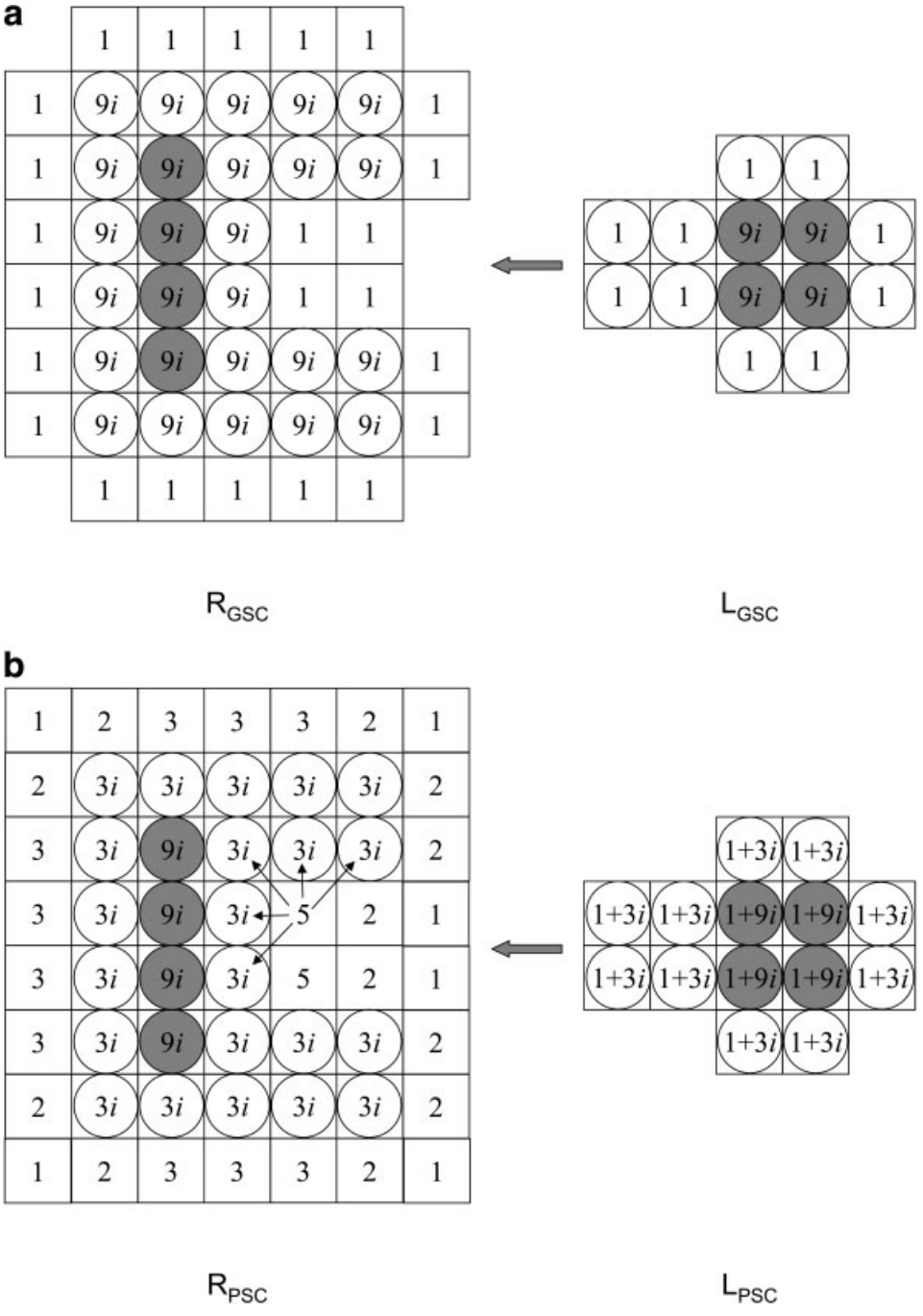

Fig. 1. 2D schematic illustration for the discrete functions (**a**) R_{GSC} and L_{GSC} used in calculating GSC (Equation 1) and (**b**) R_{PSC} and L_{PSC} for PSC (Equation 3). Protein atoms are indicated using circles, with open circles indicating surface atoms and shaded circles indicating core atoms. For clarity, we use a grid spacing that equals atom diameter and grid points whose values are 0 have been omitted from the figure. The value assigned to each grid point is indicated, with $i = \sqrt{-1}$. Grid points with open circles are in the "solvent excluded surface layer". The block arrow indicates the direction of translation for the ligand in order to achieve the optimal shape complementarity score. In **a**, grid points without any circles are in the "solvent accessible surface layer". The thickness of this layer is set to an atom diameter for illustrative purpose. In **b**, we don't define "solvent accessible surface layer"; rather, for each grid point in the open space of R_{SC}, we record the number of atoms within a distance cutoff. We have set the cutoff to be 1.5 times atom diameters for illustration purposes. Small arrows point out the five atoms that are within the distance cutoff of a grid and thus contribute to its score of 5.

within the cutoff. In Figure 1(b), we use small arrows to point out the five atoms that contribute to the score of a grid. It is clear from Figure 1(b) that grid points in the concave binding pocket of the receptor receive high scores, due to the large number of nearby atoms. This enables PSC to locate concave binding pockets effectively. The PSC score for the best ligand orientation indicated by a block arrow is 20.

Note that our PSC definition is impartial to the receptor/ligand assignment of input proteins, while previous shape complementarity functions typically work better when the protein with the concave binding site is designated as the receptor. Such a decision cannot be made when the binding site is not known. Since PSC's accuracy is not sensitive to the assignment, we always assign the larger protein as the receptor to improve computational speed.

Performance Evaluation

Following our previous work,[33] near-native structures or hits are defined as predictions with Root Mean Square Deviation (RMSD) below 2.5 Å after optimal superposition. Superposition and RMSD calculation only involve the C_α atoms of interface residues, which are receptor (or ligand) residues with at least one atom within 10 Å of any atoms of the ligand (or receptor).

In order to evaluate the overall performance of ZDOCK on the entire benchmark, we propose to use *success rate*; given some number of predictions being evaluated for each test case (N_P), success rate is the percentage of complexes in the benchmark for which at least one hit is ranked above N_P. Note that success rate only depends on the rank of the first hit in each complex. Therefore, it is useful for evaluating a stand-alone docking program. If post-processing will be involved, the number of hits a program can retain is also important. We introduce another measure of performance called *hit count*. First, we count the number of hits ranked above N_P in each test case. Hit count is simply the average of these counts over the benchmark.

Computational Implementation

Written in C, ZDOCK has been implemented on an IBM-SP and an SGI Origin 2000. We have also parallelized the program by distributing rotations amongst all processors, using Message Passing Interface (http://www-unix.mcs.anl.gov/mpi/index.html) and OpenMP (http://www.openmp.org/) for inter-processor communication. The average computing time with a 15° rotational sampling interval and a 128 × 128 × 128 grid is 4 minutes on a 16-processor IBM SP3.

RESULTS

Improving ZDOCK and GSC

We used a benchmark that contains 49 non-redundant test cases: 23 enzyme/inhibitor, 16 antibody/antigen, and 10 others.[44] There are 26 unbound/unbound and 23 unbound/bound test cases (indicated using the * symbol in Table I). To the best of our knowledge, this is the largest collection of diverse protein-protein docking test cases. Unlike earlier studies,[30,33] no homodimer has been included in this benchmark.

The two modifications we make to ZDOCK, using evenly distributed Euler angle sets and keeping only the best translational orientation per rotation, have significantly improved the performance of GSC. In Figure 2, success rates of our previous GSC[33] and the new GSC are plotted against N_P, the number of predictions retained for evaluation. The comparison was done on an earlier version of the benchmark, which included only 43 test cases (Table I except the last two enzyme/inhibitor, the last three antibody/antigen, and the last complex in the others category). When the algorithms were allowed to make only one prediction, the previous GSC succeeded for 3 complexes while the new GSC succeeded for only 2 complexes. However, the input protein structures for the previous GSC had not been randomly rotated, which contributed to its slightly inflated performance. For any other numbers of predictions, the new GSC performed better than the previous GSC, and the difference in success rate ranged 3–11%.

Also plotted in Figure 2 is the performance of the new GSC on all 49 test cases in the benchmark. The two new-GSC curves (43 vs. 49 test cases) are very similar to each other, indicating that our benchmark is sufficiently large and representative. This also indicates that the success rate vs. number of predictions curve is a useful measure for docking performance, since the same method scores similarly over a 14% increase of the test set.

It has been postulated that a thinner surface layer on the receptor would be less tolerant to clashes and, therefore, might improve the stringency of shape complementarity. Gabb et al. indicated that using thinner surface (1.2 vs. 1.5 Å) significantly improves the rankings of top hits.[24] We have thoroughly examined the impact of the surface thickness T on docking performance. Thin surface layers ($T < 2$ Å) performed poorly, with success rates less than half of that obtained with $T = 3.4$ Å at all numbers of predictions. T ranging from 2 to 3.4 Å gave similar performance, with $T = 3$ Å being the best, which has been used as the default value for all GSC calculations. Gabb et al. used finer grid resolutions (0.74–0.96 Å, vs. 1.2 Å in this study). This may explain the discrepancy between their results and ours. We did not observe any improvement with higher grid resolution, despite the significantly increased computing time (data not shown).

Optimizing PSC

PSC is composed of two terms: the favorable term calculates the total number of atom pairs between the receptor and the ligand within a distance cutoff (D plus the receptor atom radius); the penalty term prevents clashes by assigning −81 to every core-core grid point overlap and −9 to every surface-surface grid point overlap. The parameters in the penalty term (−9 and −81) have been taken directly from our earlier GSC formulation. Thus, the only adjustable parameter in the PSC scoring function is the distance cutoff D. We varied D from 2.6 to 4.6 Å with a

TABLE I. Comparison Between GSC and PSC on the Benchmark

	GSC			PSC		
Complex	Number of hits[a]	Rank[b]	RMSD[c] (Å)	Number of hits[a]	Rank[b]	RMSD[c] (Å)
1CGI	3	18	1.84	10	7	2.50
1CHO	3	116	0.79	13	1	1.51
2PTC	0	—	—	5	104	1.67
1TGS	5	113	2.13	13	9	1.83
2SNI	0	—	—	0	—	—
2SIC	1	521	1.48	3	48	1.48
1CSE	0	—	—	3	492	0.91
2KAI	0	—	—	5	252	2.22
1BRC	0	—	—	4	47	1.93
1ACB	3	147	1.61	10	20	1.37
1BRS	6	18	2.2	8	24	2.34
1JTG	5	3	1.3	9	1	2.46
1MAH	0	—	—	3	126	1.17
1UGH	1	595	2.33	1	367	1.79
1DFJ	2	373	2.43	1	12	2.48
1FSS	0	—	—	1	220	1.15
1AVW	0	—	—	7	1	2.08
1PPE*	17	1	0.74	34	1	1.17
1TAB*	0	—	—	9	5	1.38
1UDI*	2	220	2.22	3	492	1.38
1STF*	5	2	0.71	4	1	0.92
2TEC*	3	161	1.17	12	3	0.50
4HTC*	8	1	1.51	7	2	2.48
1MLC	1	632	1.59	2	580	1.80
1WEJ	0	—	—	3	259	2.43
1AHW	5	3	2.15	7	3	1.29
1DQJ	0	—	—	0	—	—
1BVK	0	—	—	3	297	2.13
1FBI*	0	—	—	0	—	—
2JEL*	3	56	0.78	17	18	1.87
1BQL*	3	62	1	5	132	1.00
1JHL*	3	129	1.73	5	51	2.10
1NCA*	4	189	2.11	9	8	1.23
1NMB*	1	829	0.91	2	272	1.21
1MEL*	3	39	1.28	10	8	1.22
2VIR*	1	39	0.78	4	413	1.26
1EO8*	0	—	—	1	843	0.62
1QFU*	3	7	0.98	3	386	1.47
1IAI*	0	—	—	1	280	2.33
2PCC	0	—	—	0	—	—
1WQI	3	340	2.28	2	301	2.01
1AVZ	0	—	—	0	—	—
1MDA	0	—	—	0	—	—
1IGC*	0	—	—	1	622	1.57
1ATN*	1	390	1.21	1	619	1.15
1GLA*	1	248	1.32	0	—	—
1SPB*	5	50	1.47	10	1	0.85
2BTF*	1	41	0.85	2	19	0.91
1A0O*	3	34	2.06	0	—	—

*, unbound/bound complexes.
[a]Hits are defined as docked structures with interface C_α RMSD ≤ 2.5 Å from the crystal complex. Only the first 1,000 predictions were retained.
[b]Best rank of any hit. "-" indicates that no hit was found.
[c]RMSD for the best ranked hit. "-" indicates that no hit was found.

0.2-Å interval to investigate its impact on algorithm performance.

We plot success rate or hit count against D, at different N_P values. Smaller D performed better for smaller N_P and larger D performed better for larger N_P, although the optimal D is slightly different for success rate and hit count. For N_P = 10 or 20, the best D values were 3.2–3.6 Å for success rate and 3.6–3.8 Å for hit count. For N_P = 500 or 1,000, they were 3.6–3.8 Å for success rate and 3.8–4.2 Å for hit count. Small D (< 3.4 Å) did poorly in terms of hit

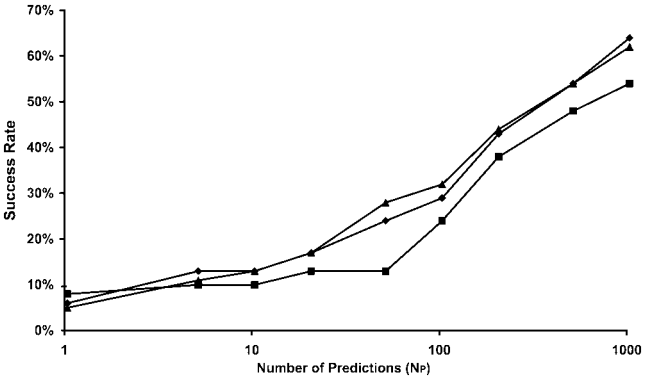

Fig. 2. The success rates of GSC with 43 (◆) and 49 (▲) test cases, and our previous GSC[33] (■) with 43 test cases are plotted against the number of predictions (N_P). The success rate is defined in Methods. It reflects the average ability of a method in ranking the first hit. Hits are predictions with interface RMSD less than 2.5 Å (see Methods for more details). The difference between the current GSC and our previous implementation is described under ZDOCK in Methods.

count, but had a lesser impact on success rate. Taken collectively, D = 3.4–3.8 Å is the best if ZDOCK is used as a stand-alone program, with a high success rate (especially at low N_P) being the chief consideration; D = 3.8 Å is the best if ZDOCK is used in combination with post-processing algorithms, since hit count (especially at high N_P) would be of primary interest. We have chosen D = 3.6 Å as the default value for subsequent PSC calculations.

Rotational Sampling

Since FFT docking algorithms perform an exhaustive search of the rotational space, it is important to investigate the impact of sampling density. Mandell et al. discovered that using angular spacing (Δ) of 6° performed significantly better than 9° for the Acetylcholinesterase/fasciculin test case while worse for Protein Kinase A/Protein Kinase Inhibitor.[26] However, no systematic analysis on a large set of test cases has been performed. Here, we compare the performance of PSC over seven Δ values (20°, 15°, 12°, 10°, 8°, 6°, and 4°), which correspond to 1,800, 3,600, 9,000, 14,400, 27,000, 54,000, and 180,000 rotations, respectively. We computed time scales linearly with the number of rotations. Using a 16-processor IBM SP3, ZDOCK spends 2 minutes per test case with Δ = 20° and 3.3 hours with Δ = 4°.

In Figure 3, we plot success rate and hit count against Δ, for various N_P values. It is apparent from Figure 3(a) that Δ = 4° has the lowest success rate for N_P larger than 100. Δ = 6° also starts to suffer when N_P becomes larger than 200. The success rates for other Δ values seem to be comparable. This observation is verified using the sign test,[49] illustrated with the following example. Compared to Δ = 15°, Δ = 4° obtained better first ranks for 6 test cases, worse for 34 test cases, and they tied for 9 test cases. If we assume that the two Δ values perform equally, the binomial distribution indicates that the probability of obtaining such a difference in performance by chance is 0.00003. We, thus, conclude that finer angular intervals tend to rank the best hits lower than coarser angular intervals.

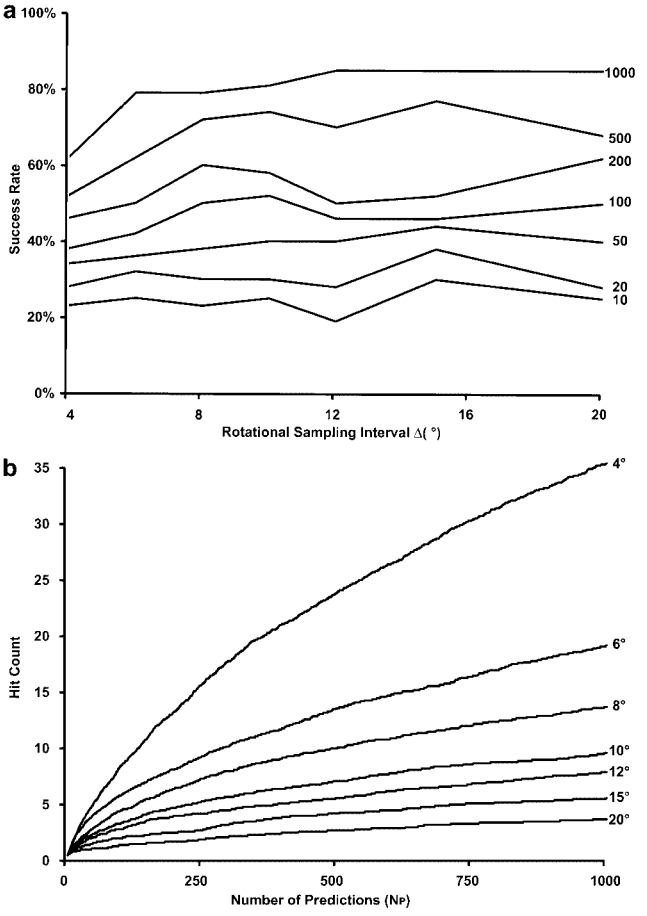

Fig. 3. The success rate (**a**) and hit count (**b**) of PSC are plotted against rotational sampling interval Δ at different N_P values: 1,000, 500, 200, 100, 50, 20, and 10. We perform a uniform rotational sampling. The angular distance between any orientation and its nearest orientation, computed using the formula in Lattman[45,46] is Δ or smaller.

The above conclusion may seem surprising. However, it can be illustrated using the following simple example. Let us assume that at a low sampling density, the first hit (called H) is ranked 2nd for a test case. This means there is one false positive (called F) that scores better than H. If we increase the sampling density 10-fold, there will be 9 new orientations (F1, F2, . . . F9) that are very similar to F, and 9 other new orientations (H1, H2, . . . H9) that are very similar to H. It is highly likely that F1, F2, . . . F9 have similar PSC scores to F, and H1, H2, . . . H9 similar to H. To a first approximation, we can assume that F, F1, F2, . . . F9 will score better than H, H1, H2, . . . H9, and, therefore, the ranking of the first hit becomes 11 at the finer sampling. Only if the scoring function is perfect will finer sampling guarantee a better performance. When the scoring function is not perfect, higher sampling density can lead to a lower success rate and higher hit count (see below).

One might decide that we should use Δ = 20°, since it takes the least amount of time. Figure 3(b) tells the other side of the story. Smaller Δ always results in more hits, at all N_P values. This could be due to the increase in total number of hits with finer sampling. To verify this, we kept

the best translational orientation per rotation and counted the total number of hits among all resulting structures. We discovered that total numbers of hits averaged over the benchmark are linearly correlated with total numbers of rotations with a correlation coefficient of 0.9999. This also implies that the number of non-hits increases linearly with total number of rotations. Thus, finer sampling increases signal and noise at the same rate. Despite this, Figure 3(b) indicates PSC is capable of ranking many more hits at the top for smaller Δ. Thus, finer rotational sampling (Δ = 6°) is recommended if ZDOCK is used as a pre-screening method, since more hits will be retained for further optimization. It is somewhat surprising that Δ = 20° performed well in success rate [Fig. 3(a)], as it appears to be too coarse. In this work, we have used Δ = 15° for comparing GSC and PSC calculations since it is rapid to compute and the conclusion should remain valid for other Δ.

For eight test cases, PSC did not find any hits within 1,000 at Δ = 15°. One possible explanation is insufficient sampling. Indeed, for 1A0O, we obtained 2 hits at Δ = 6°. However, for two other test cases (1IAI and 1EO8), even though we found one hit at Δ = 15°, we found no hit at Δ = 6°.

Comparison of PSC and GSC

Table I compares the performance of PSC and GSC. Judged by the number of hits identified in the top 1,000 predictions, PSC found more hits than GSC for 34 test cases, fewer for 6 test cases, and they tied for 9 test cases. The probability of obtaining such improvement by chance (*P* value) is less than 3×10^{-5}, computed using the sign test.[49] Judged by the rank of the first hit, PSC performed better than GSC for 32 test cases, worse for 9 test cases and the same for 8 test cases, corresponding to a *P* value of 3×10^{-4}. PSC was able to retain at least one hit in the top 1,000 for 41 test cases, compared to 30 by GSC. The improvement of PSC over GSC is seen across all three categories of test cases, although it is more apparent for enzyme/inhibitor and antibody/antigen than for others.

To compare GSC and PSC further, we plot success rate and hit count vs. number of predictions (N_P) in Figure 4. Across all N_P values, PSC has a higher success rate than GSC [Fig. 4(a)]. When each method is allowed to make only one prediction per test case, PSC succeeds for 6 test cases, 3 times as many as GSC. Figure 4(b) indicates that PSC retains many more hits than GSC throughout the entire N_P spectrum. On average, PSC detect 2.2 times as many hits as GSC. For $N_P < 20$, the ratio is increased to 2.8.

In order to investigate if PSC is more tolerant of conformational changes than GSC and, therefore, more successful for unbound docking, we performed bound docking for all co-crystal complexes. Surprisingly, PSC did much better than GSC for bound docking as well, both in success rate and in hit count, across all N_P values. The improvement is of the same magnitude for bound docking as for unbound docking. This indicates that PSC is a better measure of shape complementarity than GSC in a broad sense.

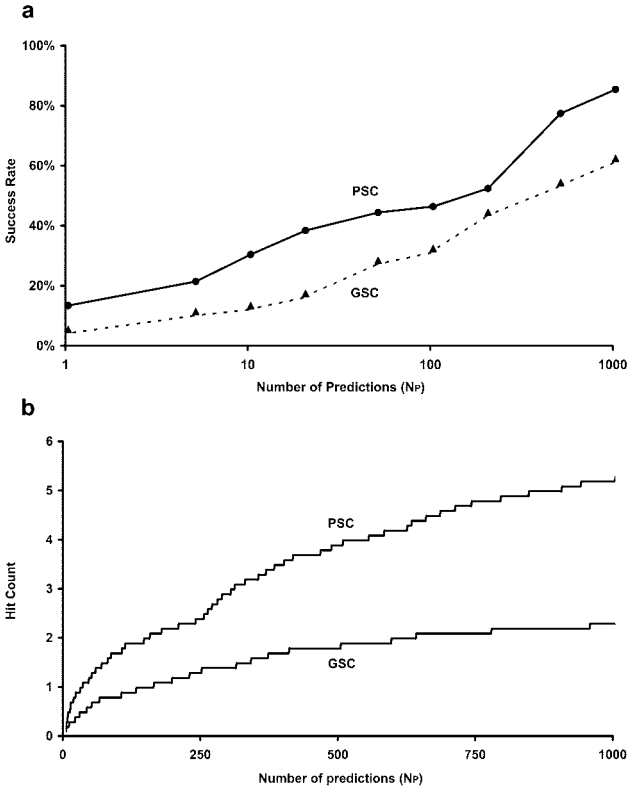

Fig. 4. The performances of PSC (● and solid line) and GSC (▲ and dashed line) for unbound docking are compared according to success rate (**a**) and hit count (**b**).

DISCUSSION

We present a novel shape complementarity scoring function PSC, which is conceptually simple and rapid to compute. We have thoroughly analyzed the impact of two parameters of PSC on algorithm performance, the distance cutoff for including favorable atom pairs and the sampling density for the rotational search. Two components are important in evaluating docking algorithms: the ability to rank hits at the top and the number of hits given some number of predictions. We propose success rate and hit count for evaluating these two components. We show that rotational intervals Δ from 20° to 8° perform similarly in terms of success rate, and Δ = 4° and 6° has a worse success rate than coarser intervals, especially at high N_P. However, finer Δ consistently generates more hits.

A drastic improvement was observed when we compared PSC to GSC; the latter has been the usual way of evaluating shape complementarity in all grid-based docking algorithms. PSC consistently ranked hits higher than GSC, produced many more hits, and the improvement was seen across all numbers of predictions and in all categories of the benchmark. The chief difference between PSC and GSC is the way they score the favorable component of shape complementarity. PSC rewards all atom pairs within a certain distance cutoff, while GSC rewards all grid points simultaneously occupied by ligand surface atoms and the

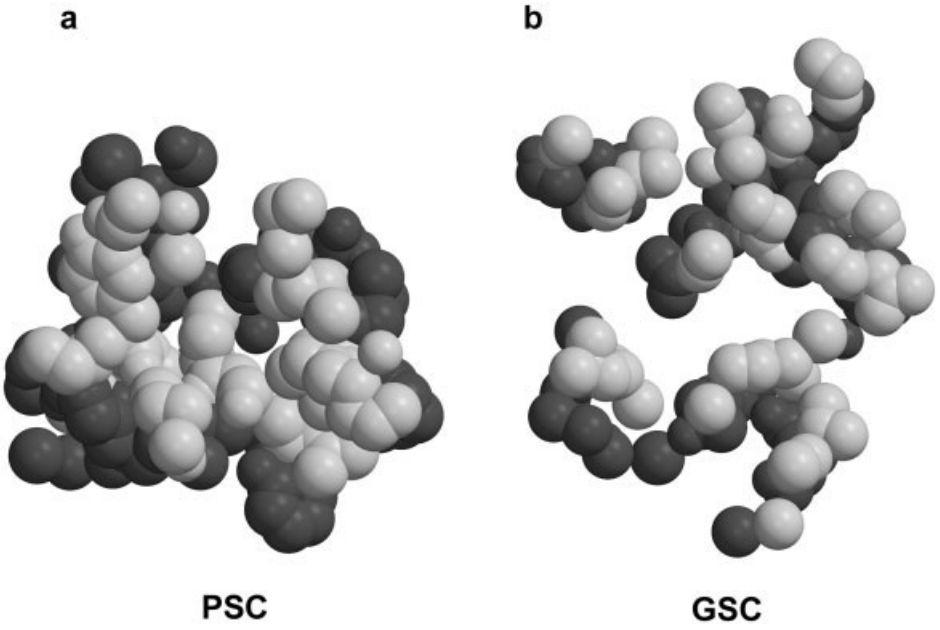

Fig. 5. The binding interface of the best prediction of 1AVW according to PSC is plotted in (**a**), compared to the binding interface of the best prediction by GSC (**b**). The interface is composed of all atoms that are within 4 Å away from the other molecule.

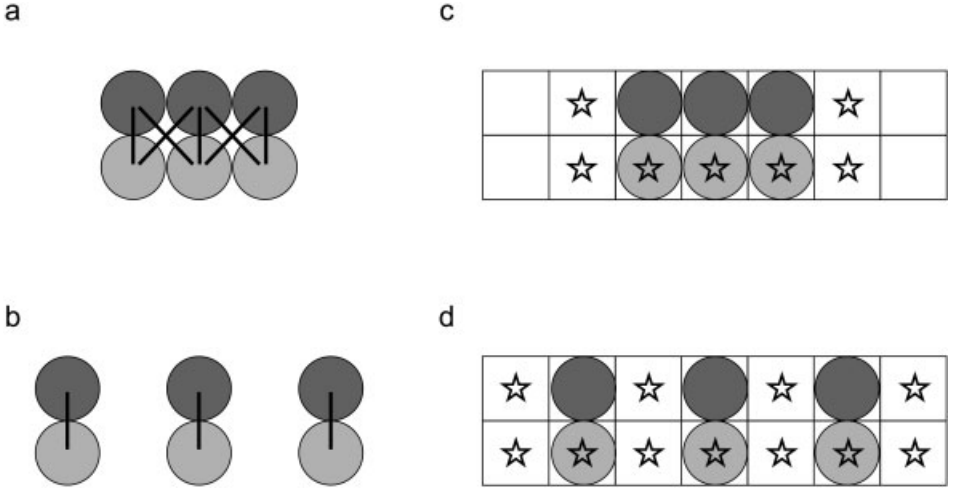

Fig. 6. Schematic illustration to compare PSC (**a**, **b**) and GSC (**c**, **d**) scores for continuous (a, c) and disjoint (b, d) interfaces. For simplicity, the interfaces are composed of the same number of receptor atoms (top; dark disks) and ligand atoms (bottom; light disks). Each line in a and b indicates one atom pair. In c and d, stars indicate solvent accessible surface of the receptor, and grid points occupied by both stars and ligand atoms are counted to compute the GSC score.

solvent accessible surface of the receptor. At first, the distinction appears subtle. We realized its implications only after comparing the top ranked structures by both methods. In Figure 5, the interface of the most favorable orientation for test case 1AVW according to PSC (a) is compared with that according to GSC (b). For clarity, only atoms within 4 Å of the other molecule are drawn. It is apparent that the PSC interface is much more contiguous than the GSC interface, and there are many cavities in the GSC interface. Upon visual inspection, one would easily conclude that the PSC structure has much better shape complementarity than the GSC structure. This pattern is seen for all test cases in the benchmark. In Figure 6, we provide an intuitive explanation for the above difference. A contiguous interface [Fig. 6(a)] is compared with a disjoint one [Fig. 6(b)] with the same number of atoms. PSC would score the contiguous interface with 7 atom pairs while the disjoint interface with only 3 atom pairs (each atom pair is indicated by a line). On the other hand, GSC would score the two interfaces equally [Fig. 6(c) and (d)] (grid points in

the solvent accessible area of the receptor are marked by stars).

Interestingly, the formulation of PSC is similar to Atomic Contact Energies (ACE) and the formulation of GSC is similar to Atomic Solvation Parameter (ASP)-based potentials. ACE and ASP have atom type specific scores while PSC and GSC treat all atom types equally. ACE and PSC are based on atom pairs, while ASP and GSC compute surface areas or grid points buried upon complex formation. Different variations of contact energies have been extensively used in protein structure prediction.[50–54] The implementation of ACE by Zhang et al. has been shown to work particularly well for calculating desolvation, both in folding and binding.[55–58] ASP-based potentials date back to the work by Eisenberg and McLachlan[59] and have found many applications in calculating desolvation energies of protein complexes. No major discrepancy between the performance of ACE and ASP has been reported, and total atom pairs and buried surface areas have been shown to correlate extremely well for protein homodimers.[60] Pioneering work by Janin and colleagues used both solvent accessible area and atom pairs within a distance cutoff to define three types of atoms at protein interfaces[61,62] clearly demonstrating the validity of both PSC and GSC approaches. Thus, the vast improvement of PSC over GSC for protein docking may seem surprising. However, it is important to keep in mind that most docked structures are false positives, many of which contain cavities at the binding interface, such as the structure shown in Figure 5(b). The simple formulation of PSC rewards contiguous interfaces, where one atom can make contacts with multiple atoms of the other molecule. As a result, PSC is particularly effective in eliminating cavity-containing false positives.

PSC is particularly good at finding concave-matching-convex interfaces, since they tend to result in more atom pairs than flat interfaces. The schematic illustration in Figure 1(b) shows that grid points at the bottom of the receptor binding pocket have the highest score (5). The active site of an enzyme is typically a deep pocket. This has contributed to PSC's outstanding performance for enzyme/inhibitor complexes. Out of the total 23 such complexes in the benchmark, PSC ranked a hit as the best structure for five complexes and in the top 10 for ten complexes. However, sometimes this property can be a drawback, especially when multiple binding sites exist and the one not being utilized is a large pocket. The glycerol-kinase/GSF-III complex (PDB code 1GLA) is an example. Not a single hit was retained by PSC in the top 1,000, even when bound structures were used. Visual inspection indicates that numerous false positives involve the deep funnel-like active site of glycerol kinase, which is unfortunately not the binding site for GSF-III. If biological information is available to indicate that the active site is not the binding site, we can easily block the center of the active site prior to the docking calculation, which frequently enables the identification of the true binding site.

For eight test cases, PSC failed to find any hits in the top 1,000. This does not pose a severe concern since shape complementarity is only one of the components of the scoring function. The improvement of PSC over GSC should set a solid foundation for additional terms such as desolvation and electrostatics. Somewhat unexpected, however, is that PSC did not find any hits in the top 1,000 orientations starting from the bound structures of three complexes: the glycerol-kinase/GSF-III complex mentioned above plus two electron transfer complexes 2PCC and 1MDA. Careful examination of the latter two complexes indicates that they have unusually poor shape complementarity (Fig. 7), with binding site similar to Figure 5b. It is apparent that there are large cavities at the binding site of both complexes (perhaps important for the electron transfer function), while other test cases are much better packed, with binding sites similar to Figure 5(a).

One might suspect the docking performance to be correlated with the extent of conformational change upon binding (indicated by the RMSD between co-crystal and unbound structures). We did not discover any correlation between the initial RMSD and the ranks of first hits or the hit counts in the top 1,000 predictions, for PSC or GSC. Similarly, we investigated whether the performance of PSC differs between unbound/unbound and unbound/bound test cases. There are 23 unbound/bound test cases in our benchmark. Intuitively, they may be easier to dock than unbound/unbound test cases since one of the starting structures is identical to the bound conformation. We performed the Mann-Whitney U-test on the hit counts in the top 1,000 predictions calculated using PSC. Briefly, all test cases were ranked in the ascending order according to the hit count. The average rank of hit count for unbound/bound test cases was 26.15, only slightly better than that for unbound/unbound test cases (23.98). The two-tailed probability of obtaining this or more extreme differences by chance, calculated using the Mann-Whitney U-test, is 0.60. We have also performed the same test using the ranks of first hits, and obtained a probability of 0.75. Thus, the performance of PSC does not differ statistically between the two classes of test cases.

In our previous study, we showed that GSC can be combined with desolvation and Coulombic electrostatics to achieve substantially improved results.[33] Similarly, desolvation and electrostatics can greatly improve upon PSC. The PSC-desolvation-electrostatitics-combined scoring function achieves higher success rate and hit count on the benchmark than the GSC-desolvation-electrostatics-combined scoring function, and a major improvement is observed for antibody/antigen test cases (Chen et al., forthcoming). Although the addition of other energy terms can further improve upon PSC, we believe that what we have learned from PSC has its own significance for two reasons. First, shape complementarity is the basic component of all scoring functions in protein docking. Some algorithms even use shape complementarity as the only component in their scoring functions.[21,22,29] The method by Ten Eyck and colleagues uses GSC and continuum electrostatics, which is more elaborate than the Coulombic electrostatics in ZDOCK. We believe that these algorithms can benefit from PSC. Second, the improvement of desolvation and

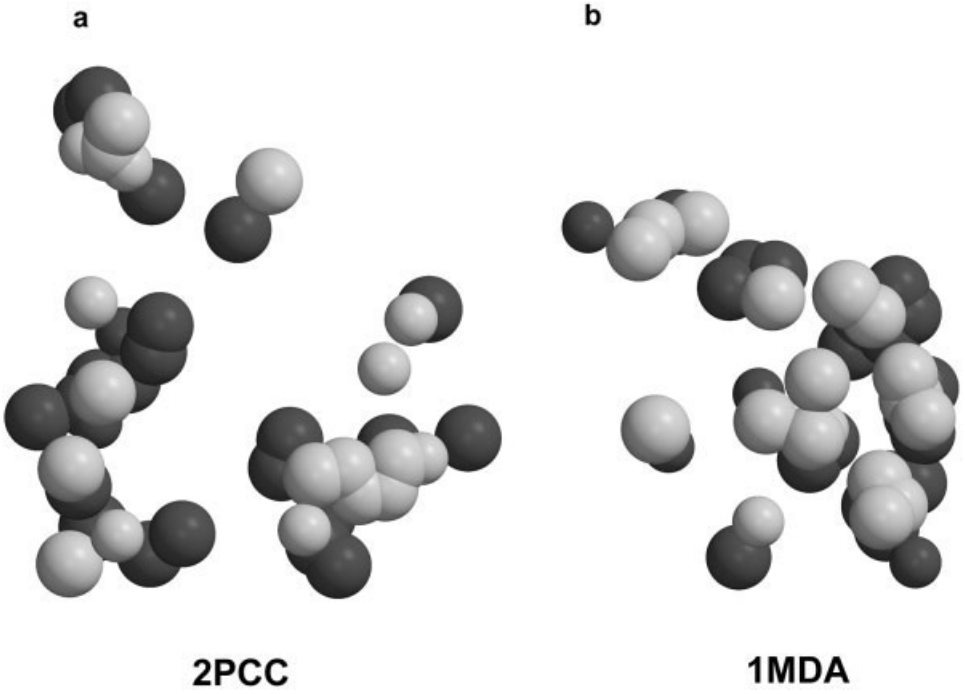

Fig. 7. The interfaces, which are composed of all atoms within 4 Å from the other molecules, are drawn for co-crystallized complex 2PCC (**a**) and 1MDA (**b**).

electrostatics over PSC is largely in the range of small N_P. An initial-stage docking algorithm such as ZDOCK must ultimately be combined with a refinement algorithm. If the refinement algorithm can handle a few thousand predictions, PSC is a competitive initial-stage scoring function. In fact, one of the best ZDOCK-refinement combinations we have developed uses PSC as the only component of the scoring function in ZDOCK.

In summary, we have developed a novel shape complementarity scoring function PSC. Careful analysis of PSC and comparison with the widely used alternative GSC indicate a drastic improvement of PSC over GSC. Since shape complementarity is the most basic ingredient of scoring functions for protein docking, our findings have important implications on the future development of docking algorithms.

ACKNOWLEDGMENTS

We thank the anonymous *Proteins* reviewers for insightful comments. We thank Dr. Julie C. Mitchell for providing uniform Euler angle sets, Julian Mintseris and Martin Frith for critically reading the manuscript, and Dr. Natalie Strynadka for providing the coordinates of BLIP crystal structures. We are grateful to the Scientific Computing Facilities at Boston University and the Advanced Biomedical Computing Center at NCI, NIH, for computing support. This work was funded by NSF grants DBI-0078194, DBI-0133834 and DBI-0116574.

REFERENCES

1. Burley SK, Almo SC, Bonanno JB, Capel M, Chance MR, Gaasterland T, Lin D, Sali A, Studier FW, Swaminathan S. Structural genomics: beyond the human genome project. Nat Genet 1999;23: 151–157.
2. Berman HM, Westbrook J, Feng Z, Gilliland G, Bhat TN, Weissig H, Shindyalov IN, Bourne PE. The Protein Data Bank. Nucleic Acids Res 2000;28:235–242.
3. Bartel PL, Roecklein JA, SenGupta D, Fields S. A protein linkage map of *Escherichia coli* bacteriophage T7. Nat Genet 1996;12:72–77.
4. Flajolet M, Rotondo G, Daviet L, Bergametti F, Inchauspe G, Tiollais P, Transy C, Legrain P. A genomic approach of the hepatitis C virus generates a protein interaction map. Gene 2000;242:369–379.
5. Rain JC, Selig L, De Reuse H, Battaglia V, Reverdy C, Simon S, Lenzen G, Petel F, Wojcik J, Schachter V, Chemama Y, Labigne A, Legrain P. The protein-protein interaction map of *Helicobacter pylori*. Nature 2001;409:211–215.
6. Walhout AJ, Sordella R, Lu X, Hartley JL, Temple GF, Brasch MA, Thierry-Mieg N, Vidal M. Protein interaction mapping in C. elegans using proteins involved in vulval development. Science 2000;287:116–122.
7. Walhout AJ, Boulton SJ, Vidal M. Yeast two-hybrid systems and protein interaction mapping projects for yeast and worm. Yeast 2000;17:88–94.
8. Ito T, Tashiro K, Muta S, Ozawa R, Chiba T, Nishizawa M, Yamamoto K, Kuhara S, Sakaki Y. Toward a protein-protein interaction map of the budding yeast: a comprehensive system to examine two-hybrid interactions in all possible combinations between the yeast proteins. Proc Natl Acad Sci USA 2000;97:1143–1147.
9. McCraith S, Holtzman T, Moss B, Fields S. Genome-wide analysis of vaccinia virus protein-protein interactions. Proc Natl Acad Sci USA 2000;97:4879–4884.
10. Uetz P, Giot L, Cagney G, Mansfield TA, Judson RS, Knight JR, Lockshon D, Narayan V, Srinivasan M, Pochart P, Qureshi-Emili A, Li Y, Godwin B, Conover D, Kalbfleisch T, Vijayadamodar G, Yang M, Johnston M, Fields S, Rothberg JM. A comprehensive analysis of protein-protein interactions in *Saccharomyces cerevisiae* [see comments]. Nature 2000;403:623–627.
11. Pandey A, Mann M. Proteomics to study genes and genomes. Nature 2000;405:837–846.

12. Weng Z, DeLisi C. Protein therapeutics: promises and challenges for the 21st century. Trends Biotechnol 2002;20:28–35.
13. Cherfils J, Janin J. Protein docking algorithms: simulating molecular recognition. Curr Opin Struct Biol 1993;3:265–269.
14. Janin J. Protein-protein recognition. Prog Biophys Mol Biol 1995;64:145–166.
15. Shoichet BK, Kuntz ID. Predicting the structure of protein complexes: a step in the right direction. Chem Biol 1996;3:151–156.
16. Sternberg MJ, Gabb HA, Jackson RM. Predictive docking of protein-protein and protein-DNA complexes. Curr Opin Struct Biol 1998;8:250–256.
17. Sternberg MJ, Gabb HA, Jackson RM, Moont G. Protein-protein docking. Generation and filtering of complexes. Methods Mol Biol 2000;143:399–415.
18. Smith GR, Sternberg MJ. Prediction of protein-protein interactions by docking methods. Curr Opin Struct Biol 2002;12:28–35.
19. Halperin I, Ma B, Wolfson H, Nussinov R. Principles of docking: an overview of search algorithms and a guid to scoring functions. Proteins 2002;47:409–443.
20. Jiang F, Kim S. Soft docking: Matching of molecular surface cubes. J Mol Biol 1991;219:79–102.
21. Katchalski-Katzir E, Shariv I, Eisenstein M, Friesem AA, Aflalo C,Vakser IA. Molecular surface recognition: determination of geometric fit between proteins and their ligands by correlation techniques. Proc Natl Acad Sci USA 1992;89:2195–9.
22. Vakser IA. Evaluation of GRAMM low-resolution docking methodology on the hemagglutinin-antibody complex. Proteins 1997; Suppl 1:226–30.
23. Vakser IA, Matar OG, Lam CF. A systematic study of low-resolution recognition in protein--protein complexes. Proc Natl Acad Sci USA 1999;96:8477–82.
24. Gabb HA, Jackson RM, Sternberg MJ. Modelling protein docking using shape complementarity, electrostatics and biochemical information. J Mol Biol 1997;272:106–20.
25. Jackson RM, Gabb HA, Sternberg MJ. Rapid refinement of protein interfaces incorporating solvation: application to the docking problem. J Mol Biol 1998;276:265–85.
26. Mandell JG, Roberts VA, Pique ME, Kotlovyi V, Mitchell JC, Nelson E, Tsigelny I, Ten Eyck LF. Protein docking using continuum electrostatics and geometric fit. Protein Eng 2001;14:105–113.
27. Mitchell JC, Phillips AT, Rosen JB, Ten Eyck LF. A coupled scanning and optimization scheme for molecular docking. In: Floudas CA, Pardalos PM, editors. Optimization in molecular biology and computational chemistry. Dordrecht: Kluwer Academic; 2000. p. 190–207.
28. Mitchell JC, Phillips AT, Rosen JB, Ten Eyck LF. Coupled optimization in protein docking. In: Istrail S, Pevzner P, Waterman M, editors. Proceedings of the Third Annual Conference in Computational Biology (RECOMB99). New York: ACM Press; 1999. p 180–184.
29. Norel R. Petrey D, Wolfson HJ, Nussinov R. Examination of shape complementarity in docking of unbound proteins. Proteins 1999;36: 307–17.
30. Palma PN, Krippahl L, Wampler JE, Moura JJ. BiGGER: A new (soft) docking algorithm for predicting protein interactions. Proteins 2000;39:372–84.
31. Ritchie DW, Kemp GJ. Protein docking using spherical polar Fourier correlations. Proteins 2000;39:178–94.
32. Gardiner EJ, Willett P, Artymiuk PJ. Protein docking using a genetic algorithm. Proteins 2001;44:44–56.
33. Chen R, Weng Z. Docking unbound proteins using shape complementarity, desolvation, and electrostatics. Proteins 2002;47:281–294.
34. Fernandez-Recio J, Totrov M, Abagyan R. Soft protein-protein docking in internal coordinates. Protein Sci 2002;11:280–91.
35. Betts MJ, Sternberg MJ. An analysis of conformational changes on protein-protein association: implications for predictive docking. Protein Eng 1999;12:271–83.
36. Connolly ML. Analytical molecular surface calculation. J. Appl. Cryst 1983;16:548–558.
37. Connolly ML. Solvent-accessible surfaces of proteins and nucleic acids. Science 1983;221:709–13.
38. Norel R, Lin SL, Wolfson HJ, Nussinov R. Molecular surface complementarity at protein-protein interfaces: the critical role played by surface normals at well placed, sparse, points in docking. J Mol Biol 1995;252:263–73.
39. Fischer D, Lin SL, Wolfson HL, Nussinov R. A geometry-based suite of molecular docking processes. J Mol Biol 1995;248:459–477.
40. Meyer M, Wilson P, Schomburg D. Hydrogen bonding and molecular surface shape complementarity as a basis for protein docking. J Mol Biol 1996;264:199–210.
41. Kuntz ID, Blaney JM, Oatley SJ, Langridge R, Ferrin TE. A geometric approach to macromolecule-ligand interactions. J Mol Biol 1982;161:269–288.
42. Shoichet BK, Kuntz ID. Protein docking and complementarity. J Mol Biol 1991;221:327–346.
43. Lorber DM, Udo MK, Shoichet BK. Protein-protein docking with multiple residue conformations and residue substitutions. Protein Sci 2002;11:1393–408.
44. Chen R, Mintseris J, Janin J, Weng Z. A protein-protein docking benchmark. Proteins (in press)
45. Lattman EE. Optimal sampling of the rotation function. Acta Crystallogr 1972;B28:1065–1068.
46. Lattman EE. Optimal sampling of the rotation function. In: Rossmann HG, editor. The molecular replacement method. New York: Gordon and Breach; 1972. p 179–185.
47. Lee B, Richards FM. The interpretation of protein structures: estimation of static accessibility. J Mol Biol 1971;55:379–400.
48. Strynadka NC, Eisenstein M, Katchalski-Katzir E, Shoichet BK, Kuntz ID, Abagyan R, Totrov M, Janin J, Cherfils J, Zimmerman F, Olson A, Duncan B, Rao M, Jackson R, Sternberg M, James MN. Molecular docking programs successfully predict the binding of a beta-lactamase inhibitory protein to TEM-1 beta-lactamase [see comments]. Nature Struct Biol 1996;3:233–9.
49. Pearson WR. Comparison of methods for searching protein sequence databases. Protein Sci 1995;4:1145–60.
50. Sippl MJ. Boltzmann's principle, knowledge-based mean fields, and protein folding. J Comp Aided Mol Des 1993;7:473–501.
51. Sippl MJ. Knowledge-based potentials for proteins. Curr Opin Struct Biol 1995;5:229–235.
52. Jernigan RL, Bahar I. Structure-derived potentials and protein simulations. Curr Opin Struct Biol 1996;6:195–209.
53. Miyazawa S, Jernigan RL. Residue-residue potentials with a favorable contact pair term and an unfavorable high packing density term, for simulation and threading. J Mol Biol 1996;256: 623–44.
54. Vajda S, Sippl MJ, Novotny J. Effective potentials for protein folding and binding. Curr Opin Struct Biol 1997;7:222–228.
55. Zhang C, Cornette JL, DeLisi C. Consistency in structural energetics of protein folding and peptide recognition. Protein Sci 1997;6: 1057–64.
56. Vasmatzis G, Zhang C, Cornette JL, DeLisi C. Computational determination of side chain specificity for pockets in class I MHC molecules. Mol Immunol 1996;33:1231–9.
57. Zhang C, Chen J, DeLisi C. Protein–protein recognition: exploring the energy funnels near the binding sites. Proteins 1999;34:255–67.
58. Zhang C, Vasmatzis G, Cornette JL, DeLisi C. Determination of atomic desolvation energies from the structures of crystallized proteins. J Mol Biol 1997;267:707–26.
59. Eisenberg D, McLachlan AD. Solvation energy in protein folding and binding. Nature (London) 1986;319:199–203.
60. Ponstingl H, Henrick K, Thornton JM. Discriminating between homodimeric and monomeric proteins in the crystalline state. Proteins 2000;41:47–57.
61. Lo Conte L, Chothia C, Janin J. The atomic structure of protein-protein recognition sites. J Mol Biol 1999;285:2177–2198.
62. Chakrabarti P, Janin J. Dissecting protein-protein recognition sites. Proteins 2002;47:334–343.